Excitonic correlation in the Mott crossover regime in Ge

Fumiya Sekiguchi[1] and Ryo Shimano[1,2]
[1]*Department of Physics, The University of Tokyo, Tokyo, 113-0033, Japan*
[2]*Cryogenic Research Center, The University of Tokyo, Tokyo, 113-0032, Japan*
(Received 3 December 2014; revised manuscript received 28 February 2015; published 6 April 2015)

Exciton Mott transition (EMT) in Ge was investigated by using optical-pump and terahertz-probe spectroscopy. From the quantitative analysis of optical conductivity and dielectric function, we evaluated the densities of unbound electron-hole pairs and excitons after the photoexcitation, from which we determined the ionization ratio of excitons α. The Mott crossover density region in Ge was elucidated from the density dependence of α in the temperature range above the critical temperature of electron-hole droplets. The $1s$-$2p$ excitonic transition energy hardly shifted with increasing density toward the EMT. Combined with the similar results recently observed in bulk Si, we suggest that the robustness of excitonic correlation against the Coulomb screening is a universal feature in bulk semiconductors in the Mott crossover regime.

DOI: 10.1103/PhysRevB.91.155202 PACS number(s): 71.30.+h, 71.35.Cc, 71.45.Gm

Insulator-to-metal transition (IMT) has long been one of the central problems in condensed matter physics, which appears in various systems ranging from doped semiconductors to strongly correlated electronic systems [1,2]. Among those systems, the photoexcited e-h system in semiconductors offers an intriguing arena for the study of IMT purely driven by the electron-electron interaction. At low temperature, electrons and holes are bound to form charge-neutral hydrogenlike quasiparticles, called excitons. When the mean interparticle distance approaches the exciton Bohr radius with increasing pair density, excitons dissociate into unbound electrons and holes, termed as e-h plasma (EHP). This transition or crossover from the insulating exciton gas to the metallic EHP is referred to as exciton Mott transition (EMT) [3–9]. EMT can be viewed as the transition (or crossover) from a strong coupling regime to a weak coupling regime in terms of the pair correlation, and the phenomenon is connected to the crossover problem between exciton Bose-Einstein condensation and e-h BCS [10–17] in the quantum degenerate regime.

EMT has been understood to occur as follows. As the e-h pair density increases, the effective Coulomb attraction between electrons and holes is weakened due to the screening effect and the Pauli-blocking effect, resulting in the reduction of the exciton binding energy E_b. In general, the screening effect plays a predominant role in the bulk system, while the Pauli blocking becomes important in lower dimensions. Concomitantly, the self-energies of single particles are reduced by many-body Coulomb interactions, known as band gap renormalization (BGR) [18,19]. The reduction of E_b and the BGR almost cancel each other, therefore the ground state ($1s$) energy of excitons hardly changes with increasing density, which physically reflects the charge neutrality of excitons. The density where E_b vanishes is called the Mott density, above which excitons cease to exist.

When the photoexcited e-h system reaches thermal quasiequilibrium, both excitons and unbound e-h pairs coexist below the Mott density [20,21]. Since the Coulomb screening should be dominated by unbound charge carriers and less contributed from charge-neutral excitons, it is important to accommodate the coexistence of excitons and unbound e-h pairs self-consistently in the theory of EMT. Therefore, the exciton ionization ratio has been identified as a relevant quantity to discuss the EMT [4,5,22,23].

Experimentally, continuous efforts have been made to reveal the EMT to date. From the photoluminescence (PL) spectroscopy, the crossover from exciton gas to EHP has been observed with increasing excitation density in a variety of materials [6,24–27]. Optical-pump and optical-probe (OPOP) spectroscopy, which probes the strength of the transition from the crystal ground state to excitonic bound states and to band-to-band continuum states after the photoexcitation, has been powerfully used to study high density phenomena including EMT and optical gain from EHP [7,8,28–30]. Recently, the common understanding for the EMT that the exciton binding energy continuously reduces with increasing density was questioned by several experiments. The signature of BGR near below the Mott density was not clearly observed in PL measurements in one-dimensional (1D) [31] and two-dimensional (2D) [26] e-h systems in GaAs. These results suggest that the broadening of the exciton and the band edge states overcome the energy shift, i.e., the real part of the single particle energy.

These PL and OPOP measurements have revealed the experimental criteria of the Mott density through the observation of broadening and suppression of excitonic levels with increasing density. However, it is difficult to determine the ionization ratio of excitons quantitatively from these measurements. On the other hand, far-infrared spectroscopy [32] and recently the terahertz time-domain spectroscopy (THz-TDS) [33–39] have been recognized as useful approaches for the investigation of EMT, since these techniques make it possible to probe the intraexcitonic transition and also the charge carrier dynamics. Importantly, combined with intense ultrafast laser pulse excitations, THz-TDS has enabled the time-resolved study on the properties of photoexcited e-h systems in a high density region. Recently, the exciton ionization ratio in bulk Si has been evaluated from the quantitative analysis of the complex dielectric function in the THz frequency range [9,40].

In light of these theoretical and experimental progresses, it is indispensable to explore the universal property of the EMT in terms of excitonic correlations by investigating the e-h systems in various material backgrounds. In this study we investigate the EMT in Ge by optical-pump and THz-probe (OPTP)

spectroscopy. Ge is a conventional indirect-gap semiconductor with a relatively large background dielectric constant of 15.6 and the exciton binding energy of $E_b = 4.2$ meV. Since the photoexcited carriers in Ge have long recombination lifetimes of the order of microseconds, they can reach a thermal quasiequilibrium condition with the lattice system within their lifetime. Because of the large band degeneracy, electron-hole droplets (EHDs) become stable below the critical temperature of $T_c \sim 6.5$ K in Ge [41,42]. The behavior of the e-h system in Ge has been intensively studied through PL and near-infrared absorption [43,44] or far-infrared absorption spectroscopy [32] to name but a few, especially in the low temperature region where excitons and electron-hole droplets (EHDs) coexist. These studies revealed the physical properties such as the critical temperature, the critical density, and the work function of EHDs, and elucidated the coexisting curve of excitons and EHDs. However, the problem of EMT below T_c of EHDs is complicated, because the liquid-gas phase separation, which has a different origin from EMT, makes the e-h system spatially inhomogeneous. To avoid the complexity associated with the formation of EHDs, we performed the OPTP spectroscopy in the temperature range above T_c where EHDs do not appear. We evaluate the ionization ratio of excitons from the spectral analysis of the complex dielectric function, and discuss the behavior of excitonic correlation in the Mott crossover regime.

The schematic experimental setup of our OPTP spectroscopy is shown in Fig. 1. For a sample we used an undoped Ge single crystal of (100) surface with the resistivity of 50 Ω cm at room temperature. The sample was mechanically polished to a thickness of 80 μm and freely mounted inside a He-gas flow cryostat. For a light source we used a Ti:sapphire regenerative amplifier with the pulse duration of 25 fs, the repetition rate of 1 kHz, and the center wavelength of 800 nm. The output from the amplifier was divided into three beams for THz generation, THz detection, and for above-gap photoexcitation of e-h pairs, respectively. For the photoexcitation, the output from an optical parametric amplifier with the wavelength of 1450 nm (855 meV) was used to pump above the indirect gap 1670 nm (744 meV) in Ge at low temperatures but below the direct gap energy of Ge 1380 nm (898 meV) [45]. At this photon energy, the penetration depth for the optical pump beam (~300 μm) [46] was larger than the sample thickness, so that the photocarrier was almost uniformly excited in the depth direction. The broadband THz-probe pulse with the frequency covering from 2 to 10 meV was generated from a 300-μm thick (110)-oriented GaP crystal by the optical rectification of the laser pulse. The THz-probe pulse transmitted after the sample was detected by the electro-optic sampling method using a 300-μm thick (110)-oriented GaP crystal. The delay time between optical pump and THz-probe pulses was fixed to 8.5 ns. The temperature difference between the photoexcited e-h system and the measured bath temperature at the sample holder was estimated as at most 2.5 K, from the emergence of EHDs in Ge ($T_c \sim 6.5$ K) at the measured temperature of 4.0 K.

Figure 2 shows the measured photoinduced changes of (a) optical conductivity $\Delta\sigma(\omega)$, and (b) dielectric function $\Delta\varepsilon(\omega)$, at 80 and 8 K. At 80 K, the spectra show the Drude-type response of the EHP. When the system was cooled to 8 K, a peak structure appeared at 3 meV in the $\Delta\sigma(\omega)$ spectrum and correspondingly a dispersive structure was identified in the $\Delta\varepsilon(\omega)$ spectrum, whose energy corresponds to the $1s$-$2p$ excitonic transition in Ge.

For a quantitative discussion we analyzed the data with Drude-Lorentz model, which describes the dielectric function as

$$\varepsilon(\omega) = \varepsilon_b + \varepsilon_D(\omega) + \varepsilon_{ex}(\omega) + \varepsilon_{lh\text{-}hh}(\omega), \quad (1)$$

$$\varepsilon_D(\omega) = -\frac{e^2 n_D}{\varepsilon_0 \mu}\left(\frac{1}{\omega^2 + i\omega\gamma_D}\right), \quad (2)$$

$$\varepsilon_{ex}(\omega) = -\frac{e^2 n_{ex}}{\varepsilon_0 \mu}\left(\frac{1}{\omega^2 - \omega_{ex}^2 + i\omega\gamma_{ex}}\right), \quad (3)$$

$$\varepsilon_{lh\text{-}hh}(\omega) = -\frac{e^2 n_{total}}{\varepsilon_0 \mu}\left(\frac{1}{\omega^2 - \omega_{lh\text{-}hh}^2 + i\omega\gamma_{lh\text{-}hh}}\right), \quad (4)$$

where ε_0 is the vacuum permittivity and $\varepsilon_b = 15.6$ is the background dielectric constant. $\mu = (1/m_e + 1/m_h)^{-1} = 0.078 m_0$ (m_0 is the bare electron mass) is the optical mass of unbound

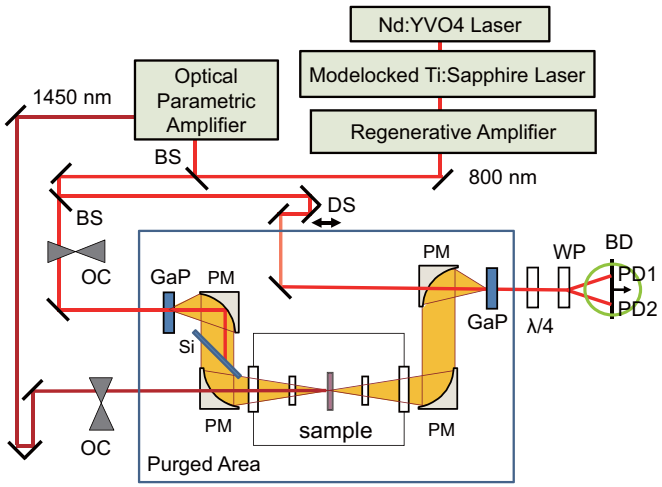

FIG. 1. (Color online) Schematic experimental setup for the optical-pump and THz-probe spectroscopy. BS: beam splitter, OC: optical chopper, DS: delay stage, PM: parabolic mirror, WP: Wollaston prism, BD: balance detector, PD: photodiode.

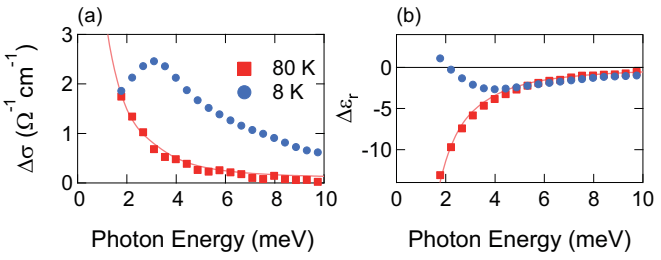

FIG. 2. (Color online) Photoinduced changes of (a) optical conductivity $\Delta\sigma$ and (b) dielectric function $\Delta\varepsilon$ at 80 and 8 K, with the total e-h pair density of 3.4×10^{15} cm^{-3}. The pump-probe delay time was fixed to 8.5 ns. Spectra at 80 K are fitted by the Drude model (solid lines).

e-h pairs, or equivalently the reduced mass of the exciton in Ge. The second term ε_D represented by Eq. (2) describes the Drude-type contribution from unbound charge carriers, with n_D and γ_D as the density and the damping constant, respectively. The third term ε_{ex} [Eq. (3)] represents the contribution from excitons by the Lorentz model, mostly contributed from $1s$-$2p$ excitonic transition, with n_{ex} and γ_{ex} as the density and the damping constant of excitons, respectively. The fourth term $\varepsilon_{lh\text{-}hh}$ [Eq. (4)] phenomenologically represents the intervalence transition, i.e., from the light-hole band (lh) to the heavy-hole band (hh), which gives a considerable strength of absorption in the THz range in the case of photoexcited Ge [47,48]. We numerically calculated the contribution of the lh-hh transition to the dielectric function with the method employed by Rose *et al.* [48], and found that in the temperature range investigated in the present work, this lh-hh contribution is reasonably represented by a simple Lorentz function with the temperature-dependent resonance frequency and the damping constant. This Lorentz function, whose spectral weight is proportional to the total density of the e-h pairs, $n_{total} = n_D + n_{ex}$, is included in the fitting function given by Eq. (1). Note that the conductivity sum rule using the simple band mass parameters does not hold in this case, where the inter- and intraband transitions give comparable contribution in the same spectral range.

Figure 3 shows examples of our fits to the experimental results at 8 and 30 K. The peak in the $\Delta\sigma$ spectra and the dispersive structure in the $\Delta\varepsilon$ spectra are reproduced by the Lorentz term [Eq. (3)] corresponding to the $1s$-$2p$ excitonic transition as shown by the shaded area in the figures. While the contribution from the lh-hh transition [Eq. (4)] also gives a Lorentz-type spectra, the damping constant is much larger than that of excitons. The spectral decomposition to these three terms was performed so that both $\Delta\sigma$ and $\Delta\varepsilon$ are reproduced simultaneously. From the fits we obtained $n_D = 6.0 \times 10^{14}$ cm^{-3}, $n_{ex} = 1.3 \times 10^{15}$ cm^{-3}, $\gamma_D = 0.86$ meV, $\gamma_{ex} = 2.9$ meV for Fig. 3(a) at 8 K, and $n_D = 1.6 \times 10^{15}$ cm^{-3}, $n_{ex} = 5.7 \times 10^{14}$ cm^{-3}, $\gamma_D = 0.72$ meV, $\gamma_{ex} = 3.2$ meV for

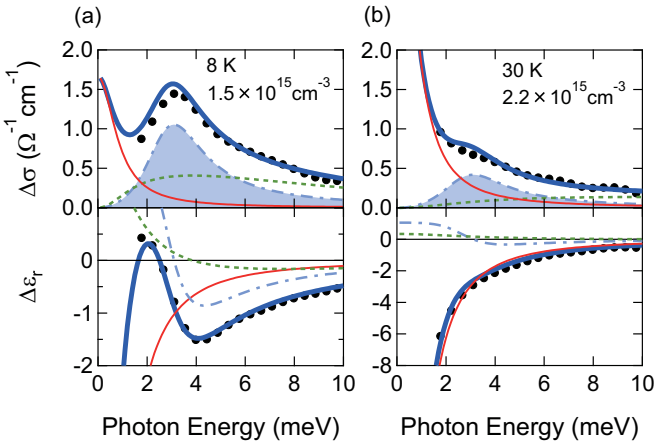

FIG. 3. (Color online) Spectral decomposition of the experimental results (black circles) at (a) 8 K and (b) 30 K. The red-thin solid line: free carrier Drude component, the blue-dotted dashed line: intraexciton transition, the green-dashed line: intervalence (lh-hh) transition, the solid blue-thick line: total sum.

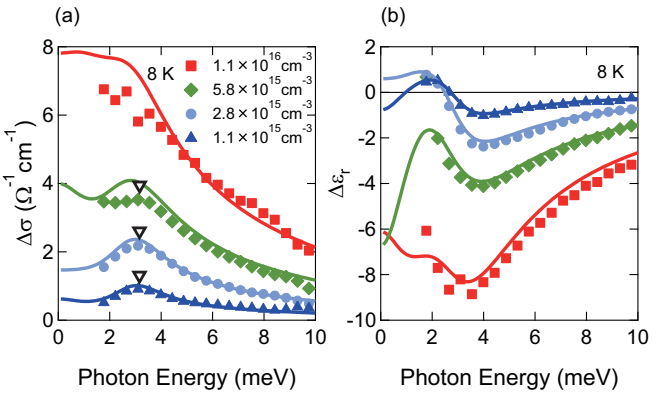

FIG. 4. (Color online) Density dependence of $\Delta\sigma$ and $\Delta\varepsilon$ at 8 K. The solid lines show the fits, and the open triangles indicate the resonance of $1s$-$2p$ intraexciton transition.

Fig. 3(b) at 30 K. The exciton ionization ratio as defined by $\alpha = n_D/n_{total}$ was determined from the fitted values of n_{ex} and n_D.

Next, in order to investigate the behavior of excitons near the Mott density, we performed the above analysis for the experimental results taken at various excitation densities and temperatures. Figure 4 shows the spectra of $\Delta\sigma$ and $\Delta\varepsilon$ at 8 K with different excitation densities. The solid lines are the fitted results with the model described above. The e-h pair densities obtained from the fits are indicated in the panels. In the low density region, the $1s$-$2p$ excitonic resonance is clearly observed around 3 meV both in the $\Delta\sigma$ and $\Delta\varepsilon$ spectra. This resonance broadens with increasing density and continuously merges into the Drude component which becomes prominent in the high density region, indicating the crossover from the exciton gas phase to metallic EHP phase. Remarkably, the $1s$-$2p$ transition energy of the excitons indicated by open triangles in the $\Delta\sigma$ spectra hardly shifts upon the Mott crossover.

Now we discuss the density dependence of the exciton ionization ratio α as shown by the solid lines in Fig. 5(a). The arrows indicate the Mott density n_{DH} at each temperature calculated from the Debye-Hückel screening of the Coulomb interaction [49]. In the high density region above n_{DH}, α increases and approaches unity with increasing density at all temperatures, which is attributed to the Mott effect. At 8 K, α increases sharply around $n_{total} \sim 1 \times 10^{16}$ cm^{-3}. This density is consistent with the Mott's criterion $n_C^{1/3} a_B = 0.26$, which leads to $n_C \sim 2 \times 10^{16}$ cm^{-3} with the exciton Bohr radius of $a_B = 106$ Å [50].

On the other hand, in the density region below n_{DH}, α does not show a monotonic decrease but remains rather constant (or even increases slightly) with decreasing density, which can be interpreted as the effect of entropy ionization [21,51]. In this density region, α increases with increasing temperature due to the thermal ionization of excitons.

First we consider the entropy-induced ionization in the low density region. We compare the behavior of α with the mass action law described by the Saha equation, which assumes the classical thermal equilibrium between excitons and unbound

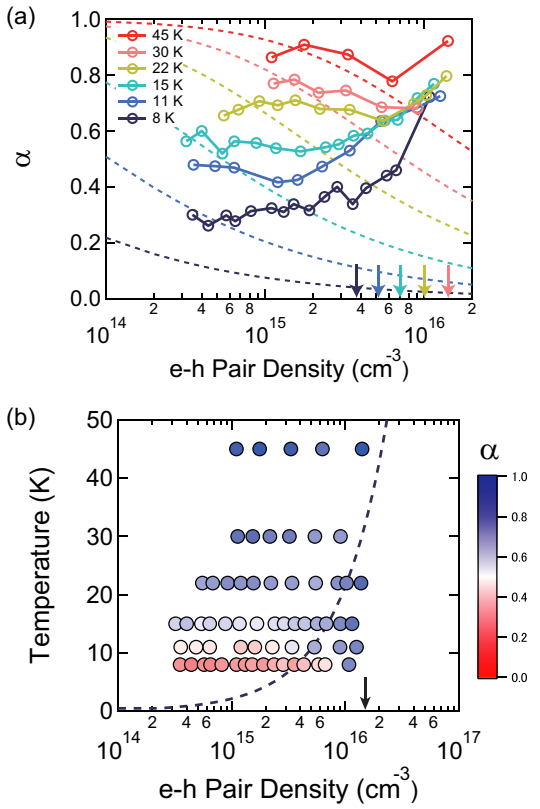

FIG. 5. (Color online) (a) The solid lines with open circles show the density dependence of exciton ionization ratio α at the indicated temperatures. The dashed lines show the ionization ratio calculated from Eq. (5), and the arrows indicate n_{DH}, the Mott density calculated with the Debye-Hückel screening, at each temperature. (b) The ionization ratio α mapped onto the phase diagram. The dashed line represents n_{DH}. The arrow indicates the Mott density given by $n_C^{1/3} a_B = 0.26$ with a_B the exciton Bohr radius.

e-h pairs, given by

$$\frac{\alpha^2}{1-\alpha} = \frac{1}{n_{\mathrm{total}}\lambda_T^3} \exp\left(\frac{-E_{\mathrm{b}}}{k_B T}\right), \tag{5}$$

where $\lambda_T = h/\sqrt{2\pi\mu_{\mathrm{d}} k_B T}$ and $\mu_{\mathrm{d}} = m_{\mathrm{de}} m_{\mathrm{dh}}/m_{\mathrm{dex}}$. The quantity λ_T takes the form of thermal de Broglie wavelength, whereas the particle mass is replaced by the e-h reduced mass. We used the density-of-state masses of the electron $m_{\mathrm{de}} = 0.22 m_0$ and of the hole $m_{\mathrm{dh}} = 0.36 m_0$. While the density-of-state mass of excitons in Ge is complicated due to the nonparabolic dispersion, we used the value of $m_{\mathrm{dex}} = 0.60 m_0$ as the geometric mean of the parameters adopted in Ref. [52]. The calculated α from the Saha equation is plotted by the dashed lines in Fig. 5(a), showing a monotonic decrease with increasing density. This behavior can be intuitively interpreted as the competition between the thermal ionization and the formation of excitons. The thermal ionization rate of excitons is considered to be linearly proportional to n_{ex} while the formation rate of excitons is proportional to $n_e n_h = n_{\mathrm{D}}^2$. Consequently, in the high density region the formation prevails against the ionization, resulting in the decrease of α.

Above 15 K, the experimentally determined α reasonably agrees with the calculation from Eq. (5) in the low density limit, indicating that the e-h systems are in the classical regime. When the density is increased, the experimental value of α starts to deviate from that of Eq. (5). With lowering temperature, this deviation becomes prominent from the lower density region, suggesting that the e-h system approaches the quantum regime.

Figure 5(b) shows the phase diagram in the n_{total} - T plane mapped by α. From this phase diagram we can grasp that the system is described as the classical e-h gas phase at high temperature and low density where excitons are ionized due to the entropy effect, while at low temperature and high density the system enters the quantum e-h gas regime where excitons are ionized due to the Mott effect. This behavior is consistent with recent theoretical studies [5,23,53]. The overall feature of the EMT seems to be consistent with the Debye-Hückel screening theory at high temperatures, although the transition is not steep and can be viewed as a crossover. At low temperatures, the onset of upturn in α is shifted to a higher density region than n_{DH}, indicating that quantum effects start to set in.

Having seen that the measured temperature and density range is located in the Mott crossover regime, we reconsider the fact that the $1s$-$2p$ excitonic transition is maintained at 3 meV upon the Mott crossover. This behavior seems to contradict the conventional picture of EMT in which continuous reduction of the exciton binding energy is expected. This result is also peculiar because the continuous shrinkage of the renormalized band gap energy E_{g}' (BGR) should result in the disappearance of the $2p$ state much below the Mott density.

One may consider that if the significant fraction of the photoexcited e-h pairs is converted into excitons, the BGR effect and the reduction of the exciton binding energy would be suppressed since the screening due to charge neutral excitons should be weak. However, this scenario contradicts the relatively large value of α evaluated in the Mott crossover regime.

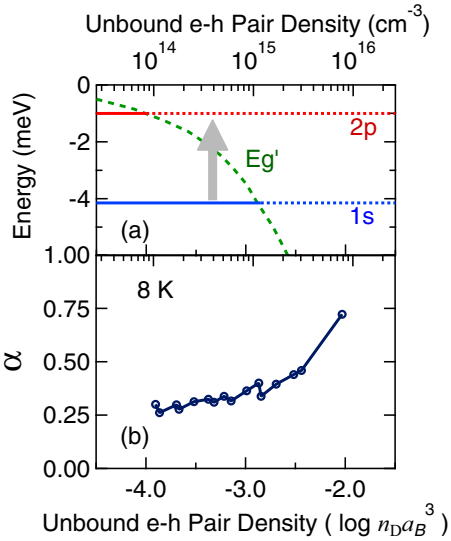

FIG. 6. (Color online) (Upper panel) A schematic picture of the suggested energy diagram, showing the sustained oscillator strength of the $1s$-$2p$ transition in the region where $E_{\mathrm{g}}' < E_{2p}$. (Lower panel) α plotted as a function of unbound e-h pair density at 8 K.

We suggest another possible explanation as schematically depicted in Fig. 6, along with the ionization ratio α at 8 K. Note that here we adopted the density of the unbound EHP (n_D) but not the total e-h pair density in the horizontal bottom axis. Also shown by the green dashed line is the renormalized band edge traced from the numerical result in Ref. [3]. The density where α exhibits a sharp upturn reasonably agrees with the density where the renormalized band edge reaches the $1s$ exciton energy in the calculated curve. If the renormalized band edge indeed reaches the $1s$ exciton energy, the sustaining oscillator strength of the $1s$-$2p$ transition across the Mott density implies that the $2p$ state continues to exist in the continuum state above the renormalized gap, presumably as a scattered state. In other words, intraexcitonic transition in the low density exciton gas continuously transfers into pair correlations in the dense metallic EHP. A similar behavior of robust excitonic correlation has been observed in bulk Si [9], where the crossover from a single-particle excitation of individual excitons to a collective excitation coupled with plasmon was suggested.

To summarize, we investigated the exciton Mott transition in Ge by the OPTP spectroscopy. The exciton ionization ratio α is derived from the quantitative analysis of the complex dielectric function, and mapped on the temperature-density phase diagram. The continuous change of α as a function of the density indicates that EMT can be viewed as a crossover in the investigated temperature range ($E_b/k_BT \geqslant 0.1$). Interestingly, the energy of the $1s$-$2p$ excitonic transition hardly shifts until it is smeared out in the broad Drude-like background in the Mott crossover density region. We consider this is a universal feature of the high density e-h systems in bulk semiconductors in the Mott crossover regime, representing the robust excitonic correlation. It will be fascinating to study how such an excitonic correlation evolves at sufficiently low temperature where the quantum degenerate phases are anticipated, and to reveal whether EMT turns into a phase transition or remains as a crossover.

We thank K. Asano, T. Suzuki, and R. Matsunaga for valuable discussion and comments. This work was partially supported by a Grant-in-Aid for Scientific Research (Grant No. 22244036) and by the Photon Frontier Network Program from MEXT, Japan.

[1] N. F. Mott, Metal-insulator transition, Rev. Mod. Phys. **40**, 677 (1968).
[2] N. F. Mott, Metal-insulator transitions, Contemporary Phys. **14**, 401 (1973).
[3] R. Zimmermann, K. Kilimann, W. D. Kraeft, D. Kremp, and G. Röpke, Dynamical screening and self-energy of excitons in the electron–hole plasma, Phys. Status Solidi (b) **90**, 175 (1978).
[4] R. Zimmermann and H. Stolz, The mass action law in two-component fermi systems revisited excitons and electron-hole pairs, Phys. Status Solidi (b) **131**, 151 (1985).
[5] T. Yoshioka and K. Asano, Exciton-mott physics in a quasi-one-dimensional electron-hole system, Phys. Rev. Lett. **107**, 256403 (2011).
[6] J. Shah, M. Combescot, and A. H. Dayem, Investigation of exciton-plasma mott transition in Si, Phys. Rev. Lett. **38**, 1497 (1977).
[7] H. Schweizer, A. Forchel, A. Hangleiter, S. Schmitt-Rink, J. P. Löwenau, and H. Haug, Ionization of the direct-gap exciton in photoexcited germanium, Phys. Rev. Lett. **51**, 698 (1983).
[8] G. W. Fehrenbach, W. Schäfer, J. Treusch, and R. G. Ulbrich, Transient optical spectra of a dense exciton gas in a direct-gap semiconductor, Phys. Rev. Lett. **49**, 1281 (1982).
[9] T. Suzuki and R. Shimano, Exciton mott transition in Si revealed by terahertz spectroscopy, Phys. Rev. Lett. **109**, 046402 (2012).
[10] P. Nozières and S. Schmitt-Rink, Bose condensation in an attractive fermion gas: From weak to strong coupling superconductivity, J. Low. Temp. Phys. **59**, 195 (1985).
[11] C. A. R. Sá de Melo, M. Randeria, and J. R. Engelbrecht, Crossover from BCS to Bose superconductivity: Transition temperature and time-dependent Ginzburg-Landau theory, Phys. Rev. Lett. **71**, 3202 (1993).
[12] For a review, see, e.g.,S. A. Moskalenko and D. W. Snoke, *Bose-Einstein Condensation of Excitons and Biexcitons: And Coherent Nonlinear Optics with Excitons* (Cambridge University Press, Cambridge, 2000).
[13] K. Yoshioka, E. Chae, and M. Kuwata-Gonokami, Transition to a Bose-Einstein condensate and relaxation explosion of excitons at sub-Kelvin temperatures, Nat. Commun. **2**, 328 (2011).
[14] G. D. Mahan, Excitons in degenerate semiconductors, Phys. Rev. **153**, 882 (1967).
[15] R. Zimmermann, Final state interactions in the gain and absorption spectra of electron-hole liquids, Phys. Status Solidi (b) **86**, K63 (1978).
[16] S. Schmitt-Rink, C. Ell, and H. Haug, Many-body effects in the absorption, gain, and luminescence spectra of semiconductor quantum-well structures, Phys. Rev. B **33**, 1183 (1986).
[17] Y. Tomio, K. Honda, and T. Ogawa, Excitonic BCS-BEC crossover at finite temperature: Effects of repulsion and electron-hole mass difference, Phys. Rev. B **73**, 235108 (2006).
[18] H. Haug and S. Schmitt-Rink, Electron theory of the optical properties of laser-excited semiconductors, Prog. Quantum Electron. **9**, 3 (1984).
[19] P. Vashishta and R. K. Kalia, Universal behavior of exchange-correlation energy in electron-hole liquid, Phys. Rev. B **25**, 6492 (1982).
[20] D. Robart, X. Marie, B. Baylac, T. Amand, M. Brousseau, G. Bacquet, G. Debart, R. Planel, and J. M. Gerard, Dynamical equilibrium between excitons and free carriers in quantum wells, Solid State Commun. **95**, 287 (1995).
[21] H. Schweizer, A. Forchel, and W. Klingenstein, Thermodynamical properties of the electron–hole system outside the region of droplet formation in germanium, Phys. Status Solidi (b) **102**, 343 (1980).
[22] D. Semkat, F. Richter, D. Kremp, G. Manzke, W. D. Kraeft, and K. Henneberger, Ionization equilibrium in an excited semiconductor: Mott transition versus Bose-Einstein condensation, Phys. Rev. B **80**, 155201 (2009).
[23] K. Asano and T. Yoshioka, Exciton–mott physics in two-dimensional electron–hole systems: Phase diagram and single-particle spectra, J. Phys. Soc. Jpn. **83**, 084702 (2014).

[24] L. Pavesi, J. L. Staehli, and V. Capozzi, Mott transition of the excitons in GaSe, Phys. Rev. B **39**, 10982 (1989).
[25] M. Nagai and M. Kuwata-Gonokami, Electron–hole liquid formation by exciton and biexciton resonant excitation in CuCl, J. Lumin. **100**, 233 (2002).
[26] L. Kappei, J. Szczytko, F. Morier-Genoud, and B. Deveaud, Direct observation of the mott transition in an optically excited semiconductor quantum well, Phys. Rev. Lett. **94**, 147403 (2005).
[27] A. Amo, M. D. Martin, L. Vina, A. I. Toropov, and K. S. Zhuravlev, Photoluminescence dynamics in GaAs along an optically induced Mott transition, J. Appl. Phys. **101**, 081717 (2007).
[28] J. Shah, R. F. Leheny, and W. Wiegmann, Low-temperature absorption spectrum in GaAs in the presence of optical pumping, Phys. Rev. B **16**, 1577 (1977).
[29] A. E. Almand-Hunter, H. Li, S. T. Cundiff, M. Mootz, M. Kira, and S. W. Koch, Quantum droplets of electrons and holes, Nature (London) **506**, 471 (2014).
[30] J. Shah, *Ultrafast Spectroscopy of Semiconductors and Semiconductor Nanostructures*, 2nd ed. (Springer, Berlin, 1999).
[31] Y. Hayamizu, M. Yoshita, Y. Takahashi, H. Akiyama, C. Z. Ning, L. N. Pfeiffer, and K. W. West, Biexciton gain and the mott transition in GaAs quantum wires, Phys. Rev. Lett. **99**, 167403 (2007).
[32] T. Timusk, Far-infrared absorption study of exciton ionization in germanium, Phys. Rev. B **13**, 3511 (1976).
[33] R. Huber, F. Tauser, A. Brodschelm, M. Bichler, G. Abstreiter, and A. Leitenstorfer, How many-particle interactions develop after ultrafast excitation of an electron–hole plasma, Nature (London) **414**, 286 (2001).
[34] R. A. Kaindl, M. A. Carnahan, D. Hagele, R. Lovenich, and D. S. Chemla, Ultrafast terahertz probes of transient conducting and insulating phases in an electron–hole gas, Nature (London) **423**, 734 (2003).
[35] R. A. Kaindl, D. Hägele, M. A. Carnahan, and D. S. Chemla, Transient terahertz spectroscopy of excitons and unbound carriers in quasi-two-dimensional electron-hole gases, Phys. Rev. B **79**, 045320 (2009).
[36] T. Suzuki and R. Shimano, Time-Resolved formation of excitons and electron-hole droplets in Si studied using terahertz spectroscopy, Phys. Rev. Lett. **103**, 057401 (2009).
[37] M. Kira and S. W. Koch, Many-body correlations and excitonic effects in semiconductor spectroscopy, Prog. Quantum Electron. **30**, 155 (2006).
[38] R. Huber, R. A. Kaindl, B. A. Schmid, and D. S. Chemla, Broadband terahertz study of excitonic resonances in the high-density regime in GaAs/$Al_xGa_{1-x}As$ quantum wells, Phys. Rev. B **72**, 161314 (2005).
[39] T. Grunwald, T. Jung, D. Köhler, S. W. Koch, G. Khitrova, H. M. Gibbs, R. Hey, and S. Chatterjee, Measurement of intraexcitonic transition signatures via THz time-domain spectroscopy: A GaAs/(AlGa)As–(GaIn)As/GaAs comparison, Phys. Status Solidi (c) **6**, 500 (2009).
[40] T. Suzuki and R. Shimano, Cooling dynamics of photoexcited carriers in Si studied using optical pump and terahertz probe spectroscopy, Phys. Rev. B **83**, 085207 (2011).
[41] G. A. Thomas, T. M. Rice, and J. C. Hensel, Liquid-gas phase diagram of an electron-hole fluid, Phys. Rev. Lett. **33**, 219 (1974).
[42] A. H. Simon, S. J. Kirch, and J. P. Wolfe, Excitonic phase diagram in unstressed Ge, Phys. Rev. B **46**, 10098 (1992).
[43] G. A. Thomas, A. Frova, J. C. Hensel, R. E. Miller, and P. A. Lee, Collision broadening in the exciton gas outside the electron-hole droplets in Ge, Phys. Rev. B **13**, 1692 (1976).
[44] G. A. Thomas, J. B. Mock, and M. Capizzi, Mott distortion of the electron-hole fluid phase diagram, Phys. Rev. B **18**, 4250 (1978).
[45] S. Zwerdling, B. Lax, L. M. Roth, and K. J. Button, Exciton and magneto-absorption of the direct and indirect transitions in germanium, Phys. Rev. **114**, 80 (1959).
[46] T. P. Maclean, *Progress in Semiconductors* (Heywood and Co. Ltd., London, 1960), Vol. 5.
[47] M. Combescot and P. Nozières, The dielectric constant and plasma frequency of *p*-type Ge like semiconductors, Solid State Commun. **10**, 301 (1972).
[48] J. H. Rose, H. B. Shore, and T. M. Rice, Infrared absorption and scattering by electron-hole droplets in Ge, Phys. Rev. B **17**, 752 (1978).
[49] F. J. Rogers, H. C. Graboske, Jr., and D. J. Harwood, Bound eigenstates of the static screened coulomb potential, Phys. Rev. A **1**, 1577 (1970).
[50] P. P. Edwards and M. J. Sienko, Universality aspects of the metal-nonmetal transition in condensed media, Phys. Rev. B **17**, 2575 (1978).
[51] J. B. Mock, G. A. Thomas, M. Combescot, Entropy ionization of an exciton gas, Solid State Commun. **25**, 279 (1978).
[52] A. Frova, G. A. Thomas, R. E. Miller, and E. O. Kane, Mass reversal effect in the split indirect exciton of Ge, Phys. Rev. Lett. **34**, 1572 (1975).
[53] G. Manzke, D. Semkat, and H. Stolz, Mott transition of excitons in GaAs-GaAlAs quantum wells, New J. Phys. **14**, 095002 (2012).